RSC Advances

PAPER

View Article Online
View Journal | View Issue

Cite this: *RSC Adv.*, 2017, **7**, 1718

Metastable intermolecular composites of Al and CuO nanoparticles assembled with graphene quantum dots†

Yue Tao,[a] Jiali Zhang,[b] Yaoyao Yang,[b] Haixia Wu,[b] Lan Hu,[c] Xiaohu Dong,[c] Jian Lu[c] and Shouwu Guo*[b]

Received 28th October 2016
Accepted 17th December 2016

DOI: 10.1039/c6ra25972c

www.rsc.org/advances

Metastable intermolecular composites (MICs) have attracted great attention during the last two decades owing to their potential applications for both civilian and military purposes. In this work, a novel category of MICs are assembled using Al and CuO nanoparticles (NPs), and graphene quantum dots (GQDs) as building blocks. It has been demonstrated that the as-assembled Al/GQDs/CuO MICs show unique energetic performance in contrast to the physical mixture of Al and CuO NPs. More specifically, the MICs assembled at relatively higher temperature and with proper Al : GQDs : CuO ratio of 20 : 1 : 90 (in weight) exhibit overall better energetic performances, including a higher heat releasing rate and larger specific heat. It was also illustrated that the specific heat amount released during the reaction can be lifted by whittling the oxide layer of the Al NPs surface, revealing that the inactive oxide layer on Al NPs should be one of the main reasons influencing the energetic performances of the MICs. Nevertheless, this work shows that the GQDs should be a useful media for MICs assembling.

Introduction

Metastable intermolecular composites (MICs), called also nanoenergetic materials (EMs) or thermite nanocomposites, can release rapidly abundant heat energy upon a thermal actuation.[1–3] Hence, the MICs have been considered as one of the most promising energetic materials for propulsion fuels, pyrotechnics, and explosives for military purposes,[1,4–7] as well as lead-free electric matches, thermal batteries and automotive air-bag propellants in civilian applications.[8,9] Generally, the MICs are composed of a fuel and oxidizer both with nanometer sizes.[10–12] In most cases, Al NPs are chosen as the fuel owing to their high energy densities, and several different metal oxide NPs, such as CuO, Fe_2O_3, Bi_2O_3, Mn_2O_3, are employed as the oxidizer in MICs.[13–19] In comparison with the bulk thermites consisting of micrometer sized or even larger Al and metal oxides particles, the MICs show superb energetic performances because their nanosized components assume usually larger surface areas, which reinforce the mass transportation and interfacial contact between the fuel and oxidizer particles. Additionally, the thickness of the passivation oxide layer on the fuel surface, and the arrangement of the nanosized fuel and oxidizer within the MICs are also the key factors influencing their energetic performances, especially, the specific heat and the heat release rate.[11,15,19–23]

During last two decades, several protocols such as physical mixing,[24–26] sol–gel processing,[20,27] high-energy ball milling,[15] and molecular self-assembling[2,9,28,29] have been developed for the preparation of MICs. Among these, the self-assembly techniques are used commonly. For instance, Gangopadhyay *et al.* assembled MICs of CuO nanorods and Al NPs with NH_4NO_3 as media.[30] Bancaud *et al.* reported a DNA-directed assembly procedure for Al/CuO MICs and found that the as-prepared MICs showing better energetic performance in comparison with the physically mixed counterparts.[9] More recently, Wang *et al.* developed an electrostatic based assembly method for preparing Al/MnO_2 MICs. Briefly, the surfaces of MnO_2 nanowires were positively charged by chemical modification with polydiallyldime-thylammonium chloride, and then were assembled with negatively charged Al NPs in aqueous solution.[31] Similarly, using poly(4-vinylpyridine) as binder, Gangopadhyay *et al.* also prepared MICs of Al NPs and CuO nanorods through a self-assembly procedure, and the as-prepared MICs showed improved energetic properties than the ones prepared with other methods.[32] However, it is worth pointing out that the media suitable for the MICs assembly procedure seems still limited.

Graphene sheets, owing to its unique single atomic layered structure, exhibit amazing physical/chemical properties,

[a]*Department of Polymer Science and Engineering, School of Chemistry and Chemical Engineering, Shanghai Jiao Tong University, Shanghai 200240, P. R. China*

[b]*Department of Electronic Engineering, School of Electronic Information and Electrical Engineering, Shanghai Jiao Tong University, Shanghai 200240, P. R. China. E-mail: swguo@sjtu.edu.cn*

[c]*Xi'an Modern Chemistry Institute, Xi'an, Shaanxi 710065, P. R. China*

† Electronic supplementary information (ESI) available. See DOI: 10.1039/c6ra25972c

including large specific surface area, high thermal conductivity, and extraordinary carrier mobility.[33,34] Graphene quantum dots (GQDs) assume the similar atomic layered structural character and properties with graphene sheets, but are less than one hundred nanometer in lateral dimensions and have more periphery carboxylic groups.[35–38] The smaller sized GQDs could also be dispersed in water and some organic solvents moderately. Putting together, the GQDs are most probably the best media candidates for MIC assembly.

In the work, we report for the first time the MICs of Al and CuO NPs assembled using GQDs as media. The composition, structure, and morphologies of as-obtained MICs were characterized complementally using high resolution microscopic and variety of spectroscopic techniques. Their energetic performances including the heat release rate and the specific heat of reaction were evaluated quantitatively. As will be shown, the heat release rate and the specific heat of reaction of the MICs assembled with GQDs are significantly higher than those of the MICs prepared simply through physical mixing of the Al and CuO NPs. In addition, the ratio of Al : GQDs : CuO, and the thickness of native oxide layer on Al NPs which may severely affect the energetic performances of MICs were explored.

Experimental

Materials

Copper(II) sulfate pentahydrate ($CuSO_4 \cdot 5H_2O$), sodium carbonate (Na_2CO_3), polyethylene glycol 400 (PEG400), ethanol, hydrogen peroxide (30% in water) (H_2O_2) were purchased from Sinopharm Chemical Reagent Co., Ltd, Shanghai, China. Sodium hydroxide (NaOH) was bought from Shanghai Lingfeng Chemical Reagent Co., Ltd, Shanghai, China. Al NPs were acquired from Xi'an Modern Chemistry Research Institute, Xi'an, China. All chemicals were used as received. Graphene oxide and GQDs were prepared following the procedures described in our previous works.[39,40]

Preparation of CuO NPs

In a typical experiment, 12 ml (0.1 M) of $CuSO_4 \cdot 5H_2O$ were added in the mixture of 150 ml of deionized water and 150 ml of ethanol that contains 60 ml of PEG400 under vigorous magnetic stirring. Then, 100 ml of saturated Na_2CO_3 aqueous solution were added dropwisely. The as-obtained solution was stirred continuously for 2 h at room temperature (~25 °C). The precipitate was separated by centrifuge and washed 3 times with deionized water and alcohol alternatively, dried at 60 °C for 12 h in vacuum oven. Finally, the solid product was grinded and calcined at 300 °C for 5 h, then 500 °C for 1 h in air to obtain the CuO NPs.

Assembling of Al/CuO MICs with GQDs

The procedure used for Al/GQDs/CuO assembling is schematically shown in Fig. 1. Specifically, 8.1 mg of Al nanoparticles was first dispersed in 50 ml deionized water under ultrasonication for 5 min at 30 °C. Then, aqueous dispersion of GQDs was added with Al : GQDs ratios of 20 : 0.5, 20 : 1, 20 : 2, 20 : 5, 20 : 10 (in weight) at pH ≈ 8, that was adjusted using diluted NaOH solution and stirred continuously for 1 h. Meanwhile, 36 mg of CuO NPs was dispersed in 100 ml deionized water under ultrasonication for 5 min at 30 °C. Finally, the CuO NPs dispersion was added into aforementioned Al/GQDs suspension and stirred vigorously for 1 h. The final ratios of Al : GQDs : CuO are of 20 : 0.5 : 90, 20 : 1 : 90, 20 : 2 : 90, 20 : 5 : 90, and 20 : 10 : 90 (in weight). At the end, the precipitate was separated by centrifuging and washed 3 times with deionized water, the solid product was dried at 50 °C for 1 h in vacuum. Notably, to compare the temperature effects, the MICs was also assembled at 10 °C through the same procedure.

Instrumental

The atomic force microscopy (AFM) images were acquired in tapping mode using a Multimode Nanoscope V scanning probe microscopy system (Bruker, USA), and AN-NSC 10AFM cantilever tips (SHNIT Co., Russia) with a force constant of ~37 N m^{-1} and resonance vibration frequency of ~300 kHz. Samples for AFM were prepared by solution casting the aqueous suspension of GQDs on a freshly cleaved mica surface and dried in air. The SEM and TEM images were acquired using Ultra 55 field emission scanning electron microscope (Zeiss, Germany) with the working voltage is 10.0 kV, and JEOL JEM-2100F transmission electron microscope (JEOL, Japan) with the operation voltage is 200 kV, and the high-resolution TEM (HRTEM) images were measured on the same instrument. The TEM specimens were prepared by placing the aqueous suspensions on the copper grids and drying under ambient condition. X-ray diffraction (XRD) patterns were recorded on a Bruker D8 Advance PC diffractometer (Bruker, Germany) using Cu/Kα radiation ($\lambda = 1.55406$ Å), with the 2θ range of 10 to 80° and the scan rate of 0.2° s^{-1}. Differential scanning calorimetry (DSC) measurements were conducted on a STA 449 F3 Jupiter (NETZSCH, Germany) at a heating rate of 10 °C min^{-1} under argon gas flow (99.999%, in purity).

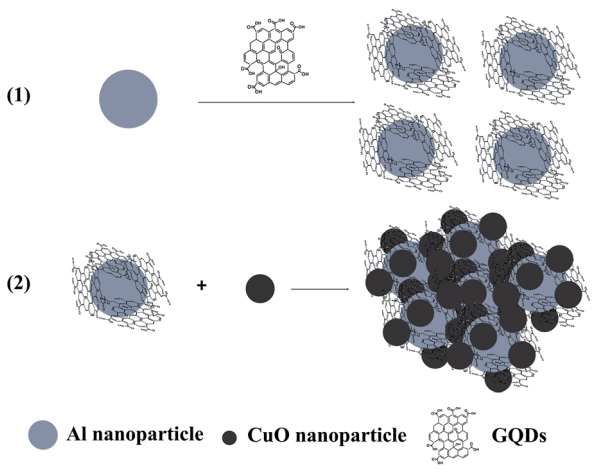

Fig. 1 Schematic representation of the assembling procedure of Al/GQDs/CuO MICs with Al and CuO NPs, and GQDs as building blocks.

Results and discussion

Characterizations of Al and CuO NPs, and GQDs

The morphology and size of Al NPs used in the work were characterized first through SEM and TEM imaging, and the results were shown in Fig. 2a and b. Clearly, the Al NPs assume well defined spherical morphology, and their average size estimated from the TEM image is of ~94 nm in diameter, but with a wide size distribution. As depicted in Fig. 2c, the sizes of as-prepared CuO NPs are ranged from 50 to 100 nm in diameter, and are aggregated somehow. The structure and composition of the CuO NPs were also verified with X-ray powder diffraction pattern (inset in Fig. 2c) which indicated that the CuO NPs assume a monoclinic crystalline phase (JCPDS standard no. 48-1548). Considering that PEG400 was used as capping reagent during the CuO NPs preparation, one may doubt the residual of the PEG400 in the CuO NPs aggregate. To clarify this, TGA data of CuO NPs was collected and depicted in Fig. S1† illustrating that the PEG400 was extirpated at 500 °C. The morphology of GQDs used in the work was studied with AFM imaging and the result is represented in Fig. 2d. The average size of GQDs is ~10 nm in diameter and the height is ~1 nm (inset in Fig. 2d), revealing the single atomic layer motif.[40,41]

Assembling of Al/GQDs/CuO MICs

It is well known that there is a native oxide layer on the surface of Al NPs,[11,21] and the GQDs used in the work containing abundant periphery carboxylic groups.[39] Thus, when Al NPs were introduced into the aqueous suspensions of GQDs, the peripheral carboxylic groups on GQDs should react with the native oxide layer on Al NPs, and the GQDs can be anchored chemically onto the Al NPs. Similarly, the as-prepared CuO NPs can also react with carboxylic groups on GQDs. Therefore, to obtain Al/GQDs/CuO MICs, after the formation of Al/GQDs, the CuO NPs were added in the reaction system under vigorous stirring. The detailed assembling procedure is schematically shown in Fig. 1. Considering that the CuO NPs and the native oxidation layer of Al NPs can be decomposed in both basic and acidic reaction systems that may affect further the formation of MICs,[42] the pH value of the reaction system was kept at ~8 during the MICs assembling. On the other hand, the assembling of Al NPs, GQDs, and CuO NPs may also be originated from the electrostatic interaction among them. To clarify the assumption, the zeta potentials of Al NPs, GQDs and CuO NPs at different pH values were measured (Fig. S2†). It shows that Al NPs and GQDs are negatively charged, CuO NPs are positively charged at pH 8, implying the electrostatic interaction is not dominating factor for the MICs assembling. To evaluate the effect of temperature on the Al/GQDs/CuO assembling, two different kinds of MICs were assembled at 10 °C and 30 °C with other conditions be the same. For comparisons, the MICs with Al : GQDs : CuO ratios of 20 : 0.5 : 90, 20 : 2 : 90, 20 : 5 : 90, 20 : 10 : 90 (in weight) were also prepared.

Fig. 3a and b show selectively the SEM images of the Al/GQDs/CuO MICs, with Al : GQDs : CuO ratio of 20 : 1 : 90, prepared at 10 and 30 °C, respectively. The morphologies of the two MICs are similar. In both cases, the Al NPs were surrounded with the relatively smaller CuO NPs which is different from the physical mixture of Al and CuO NPs without GQDs (Fig. S3a†). This implies that the GQDs do play a key role for the assembling of the Al and CuO NPs. Notably, the all as-prepared MICs with different Al : GQDs : CuO ratio assume similar morphologies, Fig. 3b and S3.† The hyperfine structure of the MICs was further elaborated using the high resolution TEM (Fig. 3d). The inter plane lattice constants fit well with Al and CuO crystals, respectively. More significantly, GQDs aggregates can be

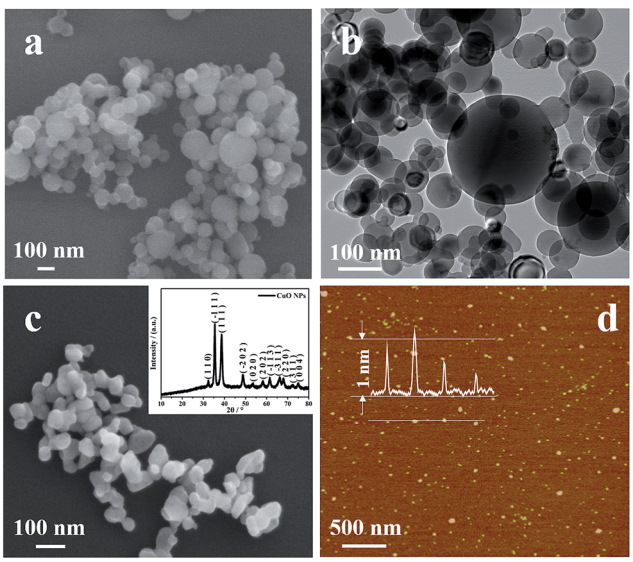

Fig. 2 (a) SEM, and (b) TEM images of Al NPs, respectively. (c) SEM image of the as-prepared CuO NPs. Inset in (c) shows the XRD pattern of the CuO NPs. (d) AFM image of GQDs deposited on freshly cleaved mica substrate. Inset in (d) is the height profile of GQDs.

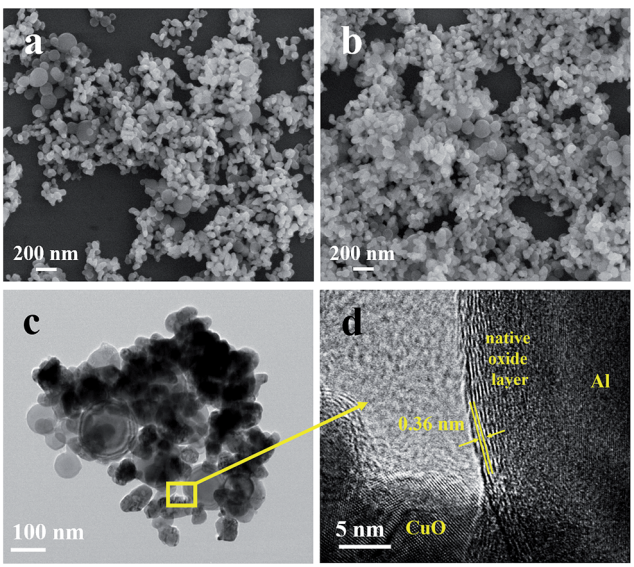

Fig. 3 (a) SEM image of Al/GQDs/CuO MICs with Al : GQDs : CuO ratio of 20 : 1 : 90 and assembled at 10 °C. (b–d) SEM, TEM, HRTEM images of the Al/GQDs/CuO MICs assembled at 30 °C.

observed clearly between Al and CuO NPs, and the *d*-spacing between the GQDs sheets is around 0.36 nm, very close to that of the graphite (0.34 nm).[43] This result provides a direct evidence of the formation of Al/GQDs/CuO MICs.

Energetic performances of as-assembled Al/GQDs/CuO MICs

To evaluate the energetic performances of the as-assembled Al/GQDs/CuO MICs, including mainly the specific heat of the reaction and the heat release rate, the DSC curves of the MICs were acquired and shown in Fig. 4. The specific heat estimated from the DSC data for the Al/GQDs/CuO MICs with Al : GQDs : CuO ratio of 20 : 1 : 90 assembled at 10 °C and 30 °C can reach to 1001.3 and 1054.0 J g^{-1}, respectively, which are much higher than those of the physically mixed Al and CuO NPs, 394.2 J g^{-1}, and also the physically mixed Al, GQDs and CuO NPs, 475.9 J g^{-1} (Fig. S4†). Comparably, the specific heat of the MICs assembled at 30 °C seems larger than that of the one prepared at 10 °C, revealing that the MICs assembled at relatively high temperature assume better energetic performance. The reason might be that at the relatively high temperature, the building blocks, GQDs, and Al, CuO NPs can be mixed more sufficiently, and thus, the fuel and oxidizer can approach to each other more easily during the reaction. Additionally, for the Al/GQDs/CuO MICs, their initial exothermal temperatures are about 50 °C lower than that of the physically mixed one. Further, the heat release rates of MICs were also enhanced dramatically. There is no exothermal peak appeared around 660 °C for Al NPs melting on the DSC curves indicating the solid–solid reaction between the Al and CuO NPs occurred, which is highly demanded for the MICs (thermite). This might be raised from the single atomic layered character and also the pronounced thermal conductivity of GQDs.[44,45]

To get insight into the effect of the GQDs on the energetic properties of the Al/GQDs/CuO MICs, the DSC data of a series of Al/GQDs/CuO MICs containing different amount of GQDs prepared at 30 °C were collected and compared. As illustrated in Fig. 4b, in general, the specific heats of the Al/GQDs/CuO MICs are always higher than that of physically mixed Al and CuO NPs. However, the fact is that the specific heat seems not continuously increased with increasing of the GQDs content in the MICs. Specifically, the specific heat released by the MICs with the Al : GQDs : CuO ratio of 20 : 0.5 : 90 (in weight) is about 811.5 J g^{-1}. When the Al : GQDs : CuO ratio is increased to 20 : 1 : 90, the specific heat reached to the maximum. With the further increasing of the GQDs content, the specific heat starts to decrease. The reasons might be that when the GQDs content is too high, the interaction between the fuel Al NPs and the oxidizer CuO NPs may be blocked somehow, thus the solid–solid reaction between Al and CuO NPs may transfer to solid–liquid reaction. On the other hand, the increase of the GQDs

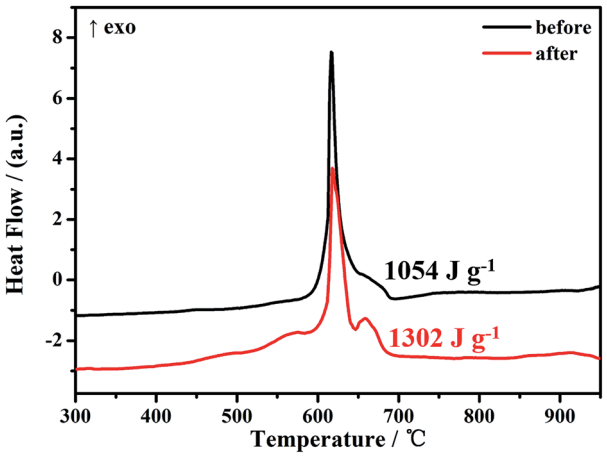

Fig. 5 DSC curves of the Al/CuO MICs assembled with GQDs which mass ratio of Al : GQDs is 20 : 1 before (black) and after (red) acid treatment, reveals the energetic performance can be improved by whittling the inactive oxide layer of Al NPs.

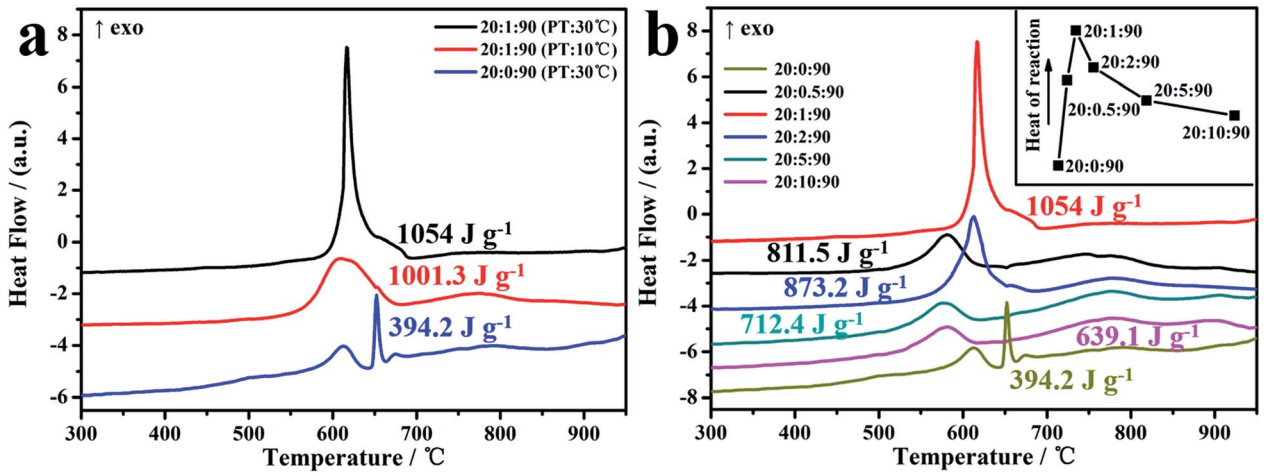

Fig. 4 (a) DSC curves of the Al/GQDs/CuO MICs assembled at 10 °C (red) and 30 °C (black) with Al : GQDs : CuO ratios of 20 : 1 : 90 (in weight), and the physically mixed Al and CuO NPs (blue) with Al : CuO ratio of 20 : 90 (in weight). (b) DSC curves of the Al/GQDs/CuO MICs assembled at 30 °C with Al : GQDs : CuO ratios of 20 : 0 : 90 (dark yellow), 20 : 0.5 : 90 (black), 20 : 1 : 90 (red), 20 : 2 : 90 (blue), 20 : 5 : 90 (dark cyan), 20 : 10 : 90 (magenta). Inset shows the relationship between the GQDs content and specific heat released during the reaction.

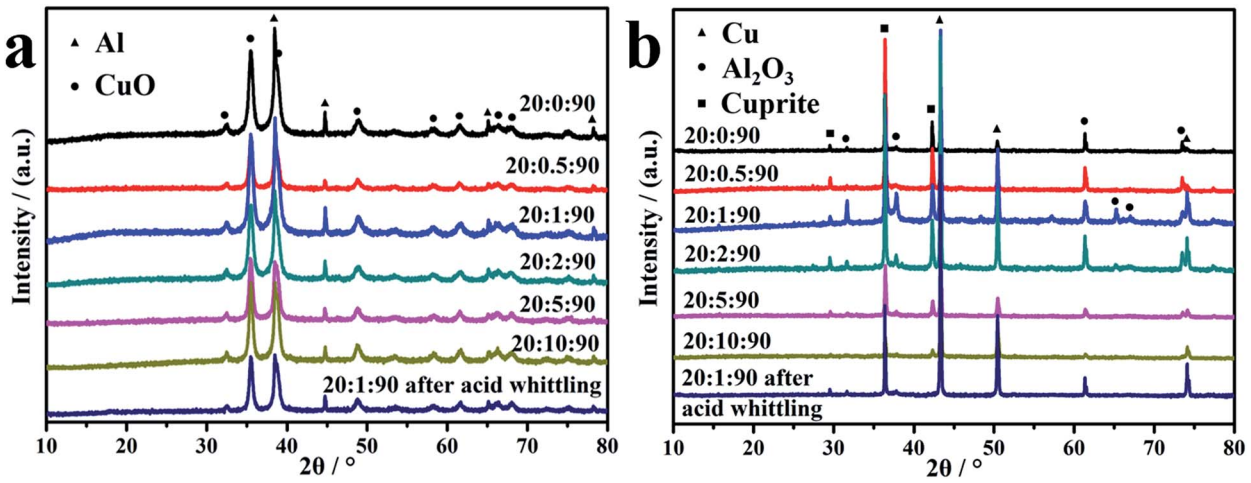

Fig. 6 X-ray diffraction patterns of Al/GQDs/CuO MICs before (a) and after (b) the reactions.

content declines the relative content of the active components (Al and CuO NPs) in the MICs which will be discussed in details later on. Additionally, the initial temperatures for the reactions of MICs are also lower than that of the physically mixed one. The detailed relationship between the GQDs content in MICs and the specific heat is summarized in the inset in Fig. 4b. Further, the narrowed FWHMs (full width at half maximum) of the exothermic peaks on DSC illustrate that the heat release rates of MICs can be accelerated with increasing of the GQDs content. The reason should be raised from the high thermal conductivity of graphene derivatives including GQDs.[44,45] Consequently, it may be concluded that using GQDs as the media for Al and CuO NPs assembling, the as-obtained MICs have more exquisite energetic performances in contrast to the physically mixed Al/CuO counterparts.

Honestly, it should be point out that the specific heats of the as-assembled MICs are far below to the theoretical specific heat of the Al/CuO thermite (3900 J g^{-1}).[9] In principle, there are several factors may contribute to the specific heat of Al/GQDs/CuO MICs. First, as mentioned above, the introduction of the inactive GQDs may be one of the reasons. However, the maximum GQDs content in the MICs with the Al : GQDs : CuO ratio of 20 : 10 : 90 is 8.3% (the content of active components is of 91.7%) (in weight), but the corresponding specific heat is only 639.1 J g^{-1}, equaling 16% of the theoretical data. This implies that the GQDs can reduce the specific heat somehow, but not the dominating factor. Second, the native oxide layer on the Al NPs can be another drawback for the effective heat release of reaction of thermite. To elaborate this, in the work, we attempt to whittle the native oxide layer on Al NPs through a quick etching procedure with diluted HCl (~0.1 M) before the MIC assembling. As depicted in Fig. S5,† the oxide layer can be whittled, but not completely because the etching reaction is conducted in aqueous solution. Nevertheless, the Al/GQDs/CuO MICs were assembled with as-whittled Al NPs and characterized. As shown in Fig. S6,† the newly assembled MICs assume similar morphology with that using original Al NPs. Remarkably, the DSC curve, Fig. 5, shows that the energetic performance of the MICs with the partially whittled Al NPs was improved dramatically. Its specific heat reaches to 1302 J g^{-1}, that is much higher than that of the MICs with original Al NPs (1054 J g^{-1}). This implies that the inactive oxide layer on Al NPs should be a major reason reducing the specific heat of the as-prepared MICs. Additionally, once the oxide layer getting thinner, the reactivity of Al NPs with CuO should be improved which is also beneficial to the increase of the heat release rate. Third, the reaction products of MICs can also affect their energetic performances. To monitor this, the XRD patterns of MICs before and after the reaction were acquired and shown in Fig. 6. Besides Al_2O_3 and Cu, cuprite was detected in the final products (Fig. 6b). This should be another reason why the specific heat of the as-assembled MICs is lower than the theoretical value of Al/CuO thermite. Because, in principle, the products of MIC after the reaction should be only Cu and Al_2O_3 reflecting the stoichiometric ratio of Al/GQDs/CuO should be optimized further.

Conclusions

In conclusion, a novel category of MICs are designed and assembled with Al and CuO NPs, and GQDs as building blocks. It was demonstrated that with GQDs as media, Al and CuO NPs can be assembled through the chemical interactions among the carboxylic groups of GQDs and the CuO and the native oxide layer on Al NPs, forming homogeneous Al/GQDs/CuO MICs. The as-assembled MICs show improved energetic performances, including the higher specific heat and faster heat release rate over the physically mixed counterparts. The specific heat of the as-assembled MICs can be tuned by varying the GQDs content, and it was illustrated that the MIC with Al : GQDs : CuO ratio of 20 : 1 : 90 has overall better energetic performances, but is still below the theoretical specific heat of Al/CuO thermite. The reason was assigned to the native oxide layer on Al NPs and also the formation of cuprite in the reaction product. The works how to whittle completely the native oxide layer on Al and to optimize the stoichiometric ratio of Al, CuO, and GQDs is

undergoing in our laboratory, and we hope to show them in our coming work.

Acknowledgements

The work was financially supported by the National "973 Program" of China (No. 2014CB260411 and 2015CB931801), the National Natural Science foundation of China (No. 11374205).

References

1 B. W. Asay, S. F. Son, J. R. Busse and D. M. Oschwald, *Propellants, Explos., Pyrotech.*, 2004, **29**, 216.
2 S. H. Kim and M. R. Zachariah, *Adv. Mater.*, 2004, **16**, 1821.
3 V. K. Patel and S. Bhattacharya, *ACS Appl. Mater. Interfaces*, 2013, **5**, 13364.
4 J. J. Granier and M. L. Pantoya, *Combust. Flame*, 2004, **138**, 373.
5 R. A. Guidotti and P. Masset, *J. Power Sources*, 2006, **161**, 1443.
6 C. R. Kaili Zhang, M. Petrantoni and N. Mauran, *J. Microelectromech. Syst.*, 2008, **17**, 832.
7 M. Petrantoni, C. Rossi, L. Salvagnac, V. Conédéra, A. Estève, C. Tenailleau, P. Alphonse and Y. J. Chabal, *J. Appl. Phys.*, 2010, **108**, 084323.
8 S. Valliappan, J. Swiatkiewicz and J. A. Puszynski, *Powder Technol.*, 2005, **156**, 164.
9 F. Séverac, P. Alphonse, A. Estève, A. Bancaud and C. Rossi, *Adv. Funct. Mater.*, 2012, **22**, 323.
10 S. F. Son, R. Yetter and V. Yang, *J. Propul. Power*, 2007, **23**, 643.
11 V. E. Sanders, B. W. Asay, T. J. Foley, B. C. Tappan, A. N. Pacheco and S. F. Son, *J. Propul. Power*, 2007, **23**, 707.
12 C. Rossi, A. Estève and P. Vashishta, *J. Phys. Chem. Solids*, 2010, **71**, 57.
13 B. S. Bockmon, M. L. Pantoya, S. F. Son, B. W. Asay and J. T. Mang, *J. Appl. Phys.*, 2005, **98**, 064903.
14 M. L. Pantoya and J. J. Granier, *J. Therm. Anal. Calorim.*, 2006, **85**, 37.
15 S. M. Umbrajkar, M. Schoenitz and E. L. Dreizin, *Thermochim. Acta*, 2006, **451**, 34.
16 T. Foley, A. Pacheco, J. Malchi, R. Yetter and K. Higa, *Propellants, Explos., Pyrotech.*, 2007, **32**, 431.
17 M. Schoenitz, S. M. Umbrajkar and E. L. Dreizin, *J. Propul. Power*, 2007, **23**, 683.
18 S. F. Son, B. W. Asay, T. J. Foley, R. A. Yetter, M. H. Wu and G. A. Risha, *J. Propul. Power*, 2007, **23**, 715.
19 J. Y. Ahn, J. H. Kim, J. M. Kim, D. W. Lee, J. K. Park, D. Lee and S. H. Kim, *Powder Technol.*, 2013, **241**, 67.
20 T. M. Tillotson, A. E. Gash, R. L. Simpson, L. W. Hrubesh, J. H. Satcher Jr and J. F. Poco, *J. Non-Cryst. Solids*, 2001, **285**, 338.
21 J. Wang, A. Hu, J. Persic, J. Z. Wen and Y. Norman Zhou, *J. Phys. Chem. Solids*, 2011, **72**, 620.
22 R. J. Jacob, G. Jian, P. M. Guerieri and M. R. Zachariah, *Combust. Flame*, 2015, **162**, 258.
23 A. Bach, P. Gibot, L. Vidal, R. Gadiou and D. Spitzer, *J. Energ. Mater.*, 2015, **33**, 260.
24 L. Wang, D. Luss and K. S. Martirosyan, *J. Appl. Phys.*, 2011, **110**, 074311.
25 J. Z. Wen, S. Ringuette, G. Bohlouli-Zanjani, A. Hu, N. H. Nguyen, J. Persic, C. F. Petre and Y. N. Zhou, *Nanoscale Res. Lett.*, 2013, **8**, 1.
26 L. Glavier, G. Taton, J.-M. Ducéré, V. Baijot, S. Pinon, T. Calais, A. Estève, M. Djafari Rouhani and C. Rossi, *Combust. Flame*, 2015, **162**, 1813.
27 A. E. Gash, T. M. Tillotson, J. Joe, H. Satcher, J. F. Poco, L. W. Hrubesh and R. L. Simpson, *Chem. Mater.*, 2001, **13**, 999.
28 J. Y. Malchi, T. J. Foley and R. A. Yetter, *ACS Appl. Mater. Interfaces*, 2009, **1**, 2420.
29 H. Wang, G. Jian, G. C. Egan and M. R. Zachariah, *Combust. Flame*, 2014, **161**, 2203.
30 R. Thiruvengadathan, A. Bezmelnitsyn, S. Apperson, C. Staley, P. Redner, W. Balas, S. Nicolich, D. Kapoor, K. Gangopadhyay and S. Gangopadhyay, *Combust. Flame*, 2011, **158**, 964.
31 Y. Yang, P. P. Wang, Z. C. Zhang, H. L. Liu, J. Zhang, J. Zhuang and X. Wang, *Sci. Rep.*, 2013, **3**, 1694.
32 R. Shende, S. Subramanian, S. Hasan, S. Apperson, R. Thiruvengadathan, K. Gangopadhyay, S. Gangopadhyay, P. Redner, D. Kapoor, S. Nicolich and W. Balas, *Propellants, Explos., Pyrotech.*, 2008, **33**, 122.
33 Y. Zhu, S. Murali, W. Cai, X. Li, J. W. Suk, J. R. Potts and R. S. Ruoff, *Adv. Mater.*, 2010, **22**, 3906.
34 X. Huang, Z. Yin, S. Wu, X. Qi, Q. He, Q. Zhang, Q. Yan, F. Boey and H. Zhang, *Small*, 2011, **7**, 1876.
35 P. He, J. Sun, S. Tian, S. Yang, S. Ding, G. Ding, X. Xie and M. Jiang, *Chem. Mater.*, 2014, **27**, 218.
36 S. H. Song, M.-H. Jang, J. Chung, S. H. Jin, B. H. Kim, S.-H. Hur, S. Yoo, Y.-H. Cho and S. Jeon, *Adv. Opt. Mater.*, 2014, **2**, 1016.
37 D. Chao, C. Zhu, X. Xia, J. Liu, X. Zhang, J. Wang, P. Liang, J. Lin, H. Zhang, Z. X. Shen and H. J. Fan, *Nano Lett.*, 2015, **15**, 565.
38 Y. Lin, R. Chapman and M. M. Stevens, *Adv. Funct. Mater.*, 2015, **25**, 3183.
39 X. Zhou, Y. Zhang, C. Wang, X. Wu, Y. Yang, B. Zheng, H. Wu, S. Guo and J. Zhang, *ACS Nano*, 2012, **6**, 6592.
40 J. Zhang, H. Yang, G. Shen, P. Cheng, J. Zhang and S. Guo, *Chem. Commun.*, 2010, **46**, 1112.
41 S. Park and R. S. Ruoff, *Nat. Nanotechnol.*, 2009, **4**, 217.
42 R. D. Letterman and S. G. Vanderbrook, *Water Res.*, 1983, **17**, 195.
43 F. Zhang, F. Liu, C. Wang, X. Xin, J. Liu, S. Guo and J. Zhang, *ACS Appl. Mater. Interfaces*, 2016, **8**, 2104.
44 A. A. Balandin, S. Ghosh, W. Bao, I. Calizo, D. Teweldebrhan, F. Miao and C. N. Lau, *Nano Lett.*, 2008, **8**, 902.
45 S. Ghosh, I. Calizo, D. Teweldebrhan, E. P. Pokatilov, D. L. Nika, A. A. Balandin, W. Bao, F. Miao and C. N. Lau, *Appl. Phys. Lett.*, 2008, **92**, 151911.